

Lattice matching and electronic structure of finite-layer graphene/*h*-BN thin films

Yuki Sakai,^{1,2} Susumu Saito,^{1,3} and Marvin L. Cohen^{2,4}

¹*Department of Physics, Tokyo Institute of Technology, 2-12-1 Oh-okayama, Tokyo 152-8551, Japan*

²*Department of Physics, University of California, Berkeley, California 94720, USA*

³*International Research Center for Nanoscience and Quantum Physics, Tokyo Institute of Technology, 2-12-1 Oh-okayama, Tokyo 152-8551, Japan*

⁴*Materials Sciences Division, Lawrence Berkeley National Laboratory, Berkeley, California 94720, USA*

(Received 28 December 2013; published 17 March 2014)

We have done a study of graphene/hexagonal boron nitride (*h*-BN) thin films within the framework of density functional theory, and find that the interlayer interaction energy of a graphene/*h*-BN monolayer thin film is inversely proportional to the layer number. This analysis based on a method which simulates the interlayer interactions in lattice-mismatched thin films shows that thin films with four or more layers can have stable lattice-matched stacking geometries. We find that the maximum value of the band gap of the lattice-matched thin films having the same layer number, but different stacking sequences, decreases with respect to the layer number, even though one can consider several different stable stacking sequences of these feasible lattice-matched thin films. In addition, the band gap can be tuned by using an external electric field. We also propose six-layer graphene/*h*-BN bilayer thin films with 99-meV band gap or graphenelike linear dispersion depending on the stacking sequences.

DOI: [10.1103/PhysRevB.89.115424](https://doi.org/10.1103/PhysRevB.89.115424)

PACS number(s): 68.65.Ac, 68.65.Pq, 73.21.Ac, 73.22.Pr

I. INTRODUCTION

Hexagonal boron nitride (*h*-BN) is well known as a good insulating substrate for graphene because of its relatively clean and flat surface [1,2]. Moreover, it has been demonstrated that graphene on a *h*-BN substrate exhibits interesting physical properties originating from their lattice mismatch (about 1.6%) [3–11]. In addition, lattice-matched finite-layer thin films [12–19] of graphene and *h*-BN as well as infinite-layer superlattices [20,21] have been intensively studied theoretically. Recently, the fabrication of graphene/*h*-BN thin films has been demonstrated experimentally [22,23], and the fabrication of an alternately stacked graphene and *h*-BN few-layer thin films by using a layer-by-layer transfer method has been also reported [24]. Such thin films can be obtained by mixing the dispersion of graphene and that of *h*-BN [25]. These experimentally fabricated thin films were considered to be lattice mismatched in contrast to the theoretically well-studied lattice-matched systems. Therefore, it is necessary to study the possibility of the lattice matching in graphene/*h*-BN thin films since the lattice matching significantly affects the electronic properties of graphene/*h*-BN heterostructures [4].

In this work, we study finite-layer thin films composed of graphene and the *h*-BN layers within the framework of density functional theory (DFT), and determine the layer-number dependence of the interlayer interaction energy of graphene/*h*-BN monolayer thin films. The number of the layers with which lattice-matched thin films become more stable than lattice-mismatched thin films is determined by utilizing twisted thin films. We also find a gap reduction with respect to the layer number, indicating the importance of intergraphene interactions as well as the sublattice symmetry breaking for considering the size of the energy gap. We also discuss the effect of an external electric field on the band gap of the graphene/*h*-BN monolayer thin films. Finally, we propose six-layer graphene/*h*-BN bilayer thin films which could repro-

duce the interesting electronic properties of graphene/*h*-BN bilayer superlattices [21].

II. COMPUTATIONAL DETAILS

In this section, we introduce the DFT methods used and the systems studied in this work.

A. DFT calculations

We perform *ab initio* calculations by using the local density approximation (LDA) within the framework of the DFT [26,27] to study the structural and electronic properties of graphene/*h*-BN thin films. The Perdew-Zunger LDA exchange correlation functionals are used [28,29]. We use the pseudopotential–plane-wave method [30–32] with a cutoff energy of 65 Ry by using the Quantum ESPRESSO package [33]. We also use van der Waals density functionals (vdW-DFs) [34] combined with ultrasoft pseudopotentials [35] to crosscheck our results. We adopt a revised version of vdW-DF [36] with Cooper’s exchange functional [37]. The cutoff energies for wave functions and charge densities are 30 and 360 Ry, respectively. A Brillouin zone integration is done on a $16 \times 16 \times 1$ k grid. We use a dense $48 \times 48 \times 1$ k grid for the electronic-structure calculations under an electric field (simulated by the use of a sawtooth-like potential). A Gaussian smearing of 0.01 Ry is used for metallic systems. We also adopt a dipole correction to remove fictitious effects caused by a dipole induced in the supercell [38]. We use XCRYSDEN to visualize the crystal structures of thin films [39].

B. Systems studied

We mainly study finite-layer thin films composed of graphene and *h*-BN monolayers. For the lattice-matched thin films, we further focus on the thin films with the *Ab*-type interface stacking geometry since this was found to be the most

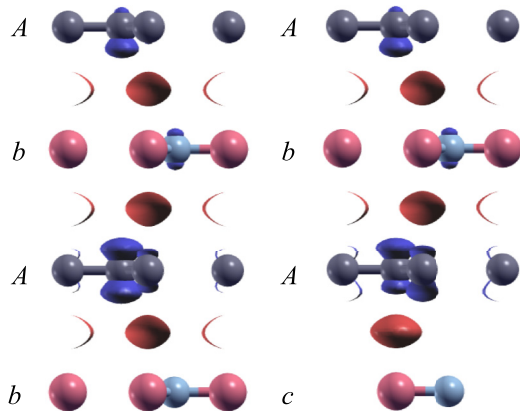


FIG. 1. (Color online) Side views of the crystal structures and differential charge densities of the $AbAb$ stacking and the $AbAc$ stacking four-layer thin films. Gray, peach, light-blue spheres illustrate carbon, boron, and nitrogen atoms, respectively. Upper case and lower case letters, respectively, represent the stacking positions of the graphene and the h -BN layers. Red and blue isosurfaces indicate 2.5×10^{-3} electron per unit volume increase and decrease, respectively.

stable stacking geometry of graphene and h -BN [4,12,20,40]. Here, the lower-case letter represents the h -BN layer. This stacking geometry is analogous to the AB stacking abundant in natural graphite [41]. Boron atoms are at the same in-plane atomic positions of one of the carbon sublattices, whereas nitrogen atoms are above or below the hollow (the center of the hexagonal ring) sites of graphene. In a major part of the systems studied in this work, the graphene layers are always AA stacked with each other while the h -BN layers can be at b or c positions. For instance, there are two possible stacking sequences (the $AbAb$ stacking and the $AbAc$ stacking shown in Fig. 1) for the four-layer thin films even when we limit our interest to the energetically stable thin films.

For lattice-mismatched thin films, first we assume no lattice mismatch between graphene and h -BN and focus on interlayer interactions. We set the in-plane lattice constant to 2.455 Å which is the average of the optimized lattice constants of the graphene (2.435 Å) and h -BN (2.475 Å) monolayer. This choice of the lattice constant is based on the previous work which showed that the optimized in-plane lattice constant of infinitely stacked graphene/ h -BN monolayer superlattice is 2.455 Å [20]. Next, we apply a twist (rotation) to the graphene/ h -BN thin films as shown in Fig. 2 to simulate the interactions between a graphene layer and a h -BN layer in lattice-mismatched thin films [3,42,43]. Here, we consider the smallest supercell (14 atoms in each layer, the twist angle between graphene and h -BN is 21.8°).¹ In the twisted thin films we studied, the graphene layers are AA stacked with each other and the h -BN layers are also aa stacked. The interlayer distances are optimized by relaxing the atomic positions in the supercell while the in-plane lattice constant is fixed.

¹We checked the total energies of seven different angles, but there are no clear trends in the total energy with respect to the twist angles (the deviation of the total energy is less than 1 meV/BC₂N).

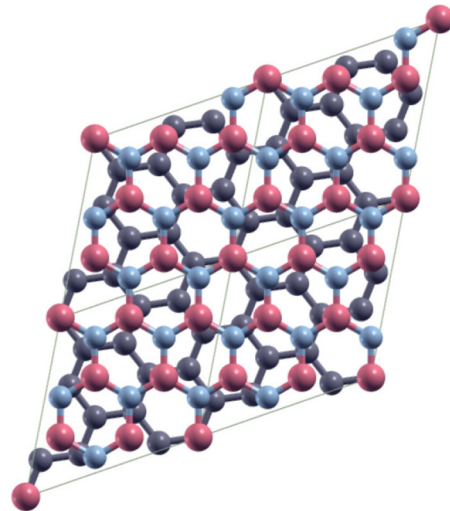


FIG. 2. (Color online) Top view of a twisted graphene/ h -BN thin film with a twist angle of 21.8° . Each unit cell has 28 atoms and four unit cells are illustrated. Graphene layers are AA stacked and h -BN layers are aa stacked with each other. The color scheme of the atoms is the same as Fig. 1.

To estimate the total energy of lattice-mismatched thin film based on the total energy of the twisted thin film, we subtract the energy loss due to the lattice matching (E_{loss}) from the total energy of the twisted graphene/ h -BN thin film. The E_{loss} is defined by

$$E_{\text{loss}} = (E_{\text{opt}}^{\text{graphene}} + E_{\text{opt}}^{\text{BN}}) - (E_{\text{matched}}^{\text{graphene}} + E_{\text{matched}}^{\text{BN}}), \quad (1)$$

where E_{opt} and E_{matched} represent the total energy of a free-standing single layer (graphene or h -BN) with an optimized in-plane lattice constant and that with the lattice constant of a lattice-matched thin film, respectively. For instance, the E_{loss} is 17 meV/BC₂N when the matched lattice constant is 2.455 Å as considered above.

III. RESULTS

This section is organized as follows: In Sec. III A, we discuss the energetics and the lattice matching in graphene/ h -BN monolayer thin films. In Secs. III B and III C, we present the electronic structures as well as the electric field effect on the band gap of these thin films. In Sec. III D, we suggest graphene/ h -BN bilayer thin films with interesting electronic properties.

A. Structural properties

Figure 3 shows the layer-number (N) dependence of the interlayer interaction energy of the graphene/ h -BN monolayer thin films. Here, we only consider the systems which have an equal number of graphene layers and h -BN layers (the number of the layers is thus always even). The red circles and green squares represent the calculated interaction energy of the lattice-matched and that of the lattice-mismatched thin films, respectively. The lines show the fitting curve of the calculated data points to the function $k/N + E_0$ where k and E_0 are fitting parameters. This $1/N$ dependence can be related to

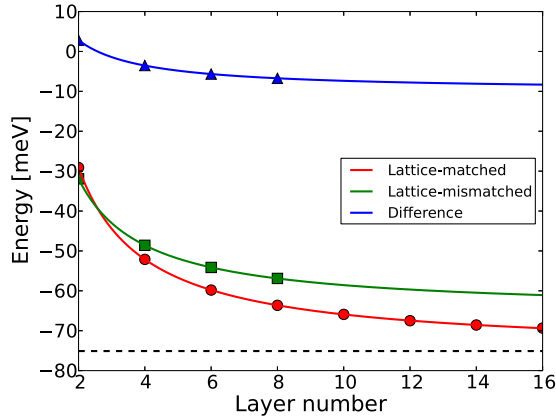


FIG. 3. (Color online) Layer-number dependence of the interlayer interaction energy (in meV). The zero of the interaction energy is the sum of the total energies of the freestanding graphene and the freestanding h -BN monolayers. The red circles and green squares represent the calculated interlayer interaction energies of the lattice-matched thin films and the estimated interaction energies of the lattice-mismatched thin films, respectively. The red and green solid lines are the fitting curves to the data points to the function $k/N + E_0$. The energy differences [the red circles (line) minus the green squares (line)] are plotted in blue triangles (line). The black dashed horizontal line shows the interaction energy of the infinite-layer graphene/ h -BN superlattice limit (75 meV/ BC_2N) [20].

the number of the interfaces of graphene and h -BN per BC_2N unit [given by $(N - 1)/(N/2)$]. The red curve (lattice-matched thin films) approaches the limit of the infinitely stacked superlattice indicated by the black dotted horizontal line in Fig. 3 as expected. The extrapolated interaction energy (E_0) of the red line in the infinite-layer limit is exactly the same as the interaction energy of the Ab -stacking graphene/ h -BN superlattice calculated in the previous work (-75 meV/ BC_2N) [20].

The blue triangles in Fig. 3 show the difference between the total energy of the lattice-matched thin films (red circles) and that of lattice-mismatched thin films (green squares). The lattice-matched thin film is 3 meV/ BC_2N less stable than the lattice-mismatched thin film in the case of the bilayer system composed of one graphene layer and one h -BN layer. This result is consistent with the experimental reports that such bilayer thin films were lattice mismatched [23]. On the other hand, the lattice-matched thin films become more stable when the system has four (4 meV/ BC_2N), six (6 meV/ BC_2N), or eight (7 meV/ BC_2N) layers. This result indicates that one needs four or more layers to obtain lattice-matched thin films.

We crosscheck the discussion above by using the vdW-DF (see Sec. II A). The interlayer interaction energies of the lattice-matched and the twisted two-layer thin films are -83 and -67 meV/ BC_2N , respectively. This result shows the inclusion of the long-range interaction gives a relatively strong interlayer interaction compared with the LDA result shown in Fig. 3. The energy loss due to lattice matching (E_{loss}) defined by Eq. (1) is now 20 meV/ BC_2N . Thus, the lattice-matched two-layer thin film is 4 meV/ BC_2N less stable than a lattice-mismatched thin film. On the other hand, lattice-matched thin films are 5 meV/ BC_2N , 8 meV/ BC_2N , and 10 meV/ BC_2N

more stable in four-, six-, and eight-layer cases, respectively, in this vdW-DF study. Therefore, the quantitative discussion on lattice matching should remain unchanged even when we consider the long-range interaction.

The shorter interlayer distance in the lattice-matched Ab -stacking thin films (3.24 Å) than the twisted thin films (3.41 Å) implies a stronger interlayer interaction in the Ab -stacking interface. The energy gain due to this strong interlayer interaction exceeds the energy loss due to lattice matching when the layer number becomes large. Lattice-matched thin films can be obtained by applying pressure as suggested in graphene/ h -BN superlattice cases [40]. Based on the energetics here, we discuss four-, six-, and eight-layer thin films in the remaining part of this paper.

B. Electronic structure

The differential electronic charge densities of the $AbAb$ -stacking and the $AbAc$ -stacking thin films are shown in Fig. 1. All the carbon atoms and the nitrogen atoms lose electrons while the interlayer spaces gain electrons. The boron atoms also lose electrons but the loss can not be seen in the figure since the amount is smaller than those of the carbon and the nitrogen atoms. The implication of the increase of electrons in the interlayer spaces can be speculated to be that the interlayer bonding is at least partially of chemical nature rather than ordinary van der Waals interactions. The charge density decreases of two carbon sublattices in the lower graphene layer are inequivalent in the $AbAb$ -stacking thin film because one of the carbon sublattices is in-between two boron atoms whereas the other carbon sublattice is in-between two hollow sites of the adjacent h -BN layers. A similar but small inequivalent charge density reduction can be seen in upper graphene layers of both the $AbAb$ -stacking and the $AbAc$ -stacking thin films. On the other hand, the two carbon sublattices lose almost the same amount of electrons in the $AbAc$ -stacking thin film since every carbon sublattice is in-between a boron atom and a hollow site of the adjacent h -BN layers.

The difference in the charge density of two different carbon sublattices breaks sublattice symmetry and induces a band gap around the K point in the first Brillouin zone. The band structures of the four-layer thin films with different stacking sequences (the $AbAb$ stacking and the $AbAc$ stacking) are shown in Fig. 4. The red arrows represent the band-gap opening due to the broken sublattice symmetry. The upper and the lower arrows in the band-structure plot of the $AbAb$ -stacking thin film indicates the gap opening in the upper and the lower graphene layers (see Fig. 1), respectively. In a similar fashion, the upper and lower arrows in the band-structure plot of the $AbAc$ -stacking thin film correspond to the band gap in the lower and the upper graphene layers.

The band gaps are 7 and 48 meV in the $AbAb$ -stacking and the $AbAc$ -stacking thin films, respectively as listed in Table I. The difference in the band gaps can be related to the hybridization between π and π^* states of the two different graphene layers. In the $AbAb$ -stacking thin film, the π state of the upper graphene layer has overlap with the π^* state of the lower graphene layer. Similarly, the π state of the lower graphene layer hybridizes with the π^* state of the upper graphene layer in the $AbAc$ -stacking thin film. The overlap

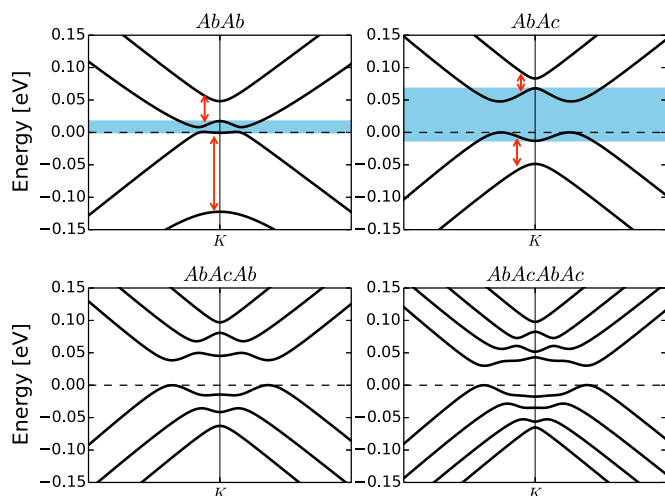


FIG. 4. (Color online) The band structure of the four layer (*AbAb*-stacking and *AbAc*-stacking) graphene/*h*-BN thin film in the vicinity of the high-symmetry *K* point in the first Brillouin zone (top panels). The red two-direction arrows show the gap opening caused by the broken sublattice symmetry. The blue backgrounds show the expected overlap between the electronic states of two graphene layers. The labels of the panels show the stacking sequences. The valence band top is set to the zero energy (the horizontal dashed line). The band structures of six-layer (*AbAcAb*-stacking) and eight-layer (*AbAcAbAc*-stacking) thin films are also shown in the bottom panels.

region (the blue background in Fig. 4) in the *AbAb*-stacking thin film is smaller than that of the *AbAc*-stacking thin film, which is consistent with the size of the band gaps.

The electronic structures of six-layer (*AbAbAb*-stacking) and eight-layer (*AbAcAbAc*-stacking) thin films are also shown in Fig. 4. There are three (*AbAbAb*, *AbAbAc*, and *AbAcAb*) and six (*AbAbAbAb*, *AbAbAbAc*, *AbAbAcAb*, *AbAbAcAc*, *AbAcAbAc*, and *AbAcAcAb*) possible stable stacking sequences for the six- and eight-layer thin films, respectively. We plot only the electronic structures of the above two thin films because both the *AbAcAb*-stacking and the *AbAcAbAc*-stacking thin films, respectively, have the largest band gaps (38 and 30 meV) among six- and eight-layer thin

TABLE I. Band gaps (in meV) of various graphene/*h*-BN monolayer thin films. Two, three, and six different stacking sequences of four-, six-, and eight-layer thin films are respectively listed.

Layer number	Stacking sequence	Band gap
4	<i>AbAb</i>	7
	<i>AbAc</i>	48
6	<i>AbAbAb</i>	0
	<i>AbAbAc</i>	14
	<i>AbAcAb</i>	38
8	<i>AbAbAbAb</i>	0
	<i>AbAbAbAc</i>	6
	<i>AbAbAcAb</i>	22
	<i>AbAbAcAc</i>	0
	<i>AbAcAbAc</i>	30
	<i>AbAcAcAb</i>	9

films as listed in Table I. This result implies a monotonic reduction of these largest band-gap values (the largest among thin films with different stacking sequence and the same layer number) with respect to the layer number. The overlaps between the electronic states of graphene layers in both six- and eight-layer thin films are larger than those in the four-layer systems discussed above. However, these states have overlap with a multiple number of states. The hybridization among the states of the graphene layers (intergraphene interaction) is considered to reduce the band-gap size. In fact, the electronic properties of the infinitely stacked graphene/*h*-BN monolayer superlattices are metallic because of the band dispersion along the direction perpendicular to the layers [20]. Thus, this band-gap reduction trend is also consistent with the infinite-layer limit.

C. Electric field effect

Figure 5 shows the electric field effect on the band gap of the *AbAb*-stacking (the blue circles) and the *AbAc*-stacking (the red squares) four-layer thin film. The electric field shifts the relative potential of each layer, and thus alters the overlap between π and π^* states. The band-gap modulations are caused by this change in the overlap of the states, in the same manner as the discussion in Sec. III B. The band gap goes to approximately zero when the overlap becomes negligible. One can tune the band gap of the thin film although there is a saturation of the band gap (begins from $\sim \pm 2$ V/nm in Fig. 5) similar to those known in the bilayer graphene [44].

The asymmetric behaviors with respect to the sign of the electric field come from the asymmetries of the structures of the thin films (all thin films have graphene-terminated side and *h*-BN-terminated side along the direction perpendicular to the layers as shown in Fig. 1). There is also another asymmetry between the electric field effects on the *AbAb*-stacking thin film and those on the *AbAc*-stacking thin film. In the positive field cases, the band gap of the *AbAb*-stacking thin film once increases and gradually decreases while the band gap of the

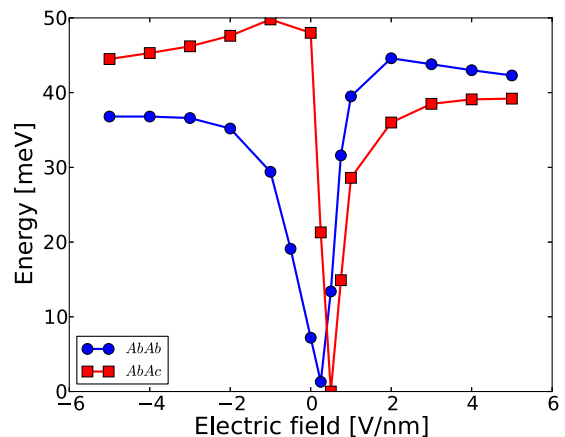


FIG. 5. (Color online) Band gaps (in meV) of the *AbAb*-stacking (blue circles) and *AbAc*-stacking (red squares) four-layer thin films with respect to the external electric field (in V/nm). The direction of the applied electric field is perpendicular to the layers and points from graphene-terminated side to *h*-BN-terminated side (the geometries are shown in Fig. 1).

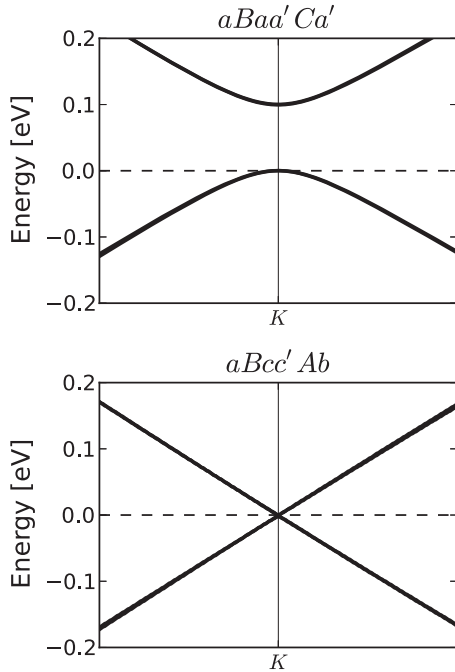


FIG. 6. Band structures of the $aBaa'Ca'$ -stacking (top panel) and the $aBcc'Ab$ -stacking (bottom panel) thin films in the vicinity of the K point in the first Brillouin zone. Two π states as well as two π^* states are almost degenerated with each other in both panels.

$AbAc$ -stacking thin film shows asymptotic behavior, and vice versa. As mentioned in Sec. III B, there is an overlap between the π state of the upper (lower) graphene layer and the π^* state of the lower (upper) graphene layer in the $AbAb$ -stacking ($AbAc$ -stacking) thin film in the zero electric field case. These initial overlaps in these two thin films are thus opposite to each other, and this leads to the asymmetric behavior.

D. Thin films with bilayer h -BN

In the previous work, it was suggested that one can fabricate stable and lattice-matched graphene/ h -BN bilayer superlattices with infinite layers. The superlattices have 100-meV band gap or a linear dispersion depending on stacking sequences [21]. The experimental fabrication of such infinitely stacked superlattices is actually difficult in spite of their interesting properties. Here, we show that such electronic properties could be realized not only in graphene/ h -BN superlattices but also in lattice-matched six-layer thin films.

We consider $aBaa'Ca'$ -stacking and $aBcc'Ab$ -stacking thin films. The prime symbol in the stacking sequences represents the exchange of the atomic positions of boron atoms and nitrogen atoms so that aa' stacking represents the stacking sequence of natural h -BN. These lattice-matched thin films are $3 \text{ meV}/(\text{BCN})_2$ more stable than lattice-mismatched systems estimated by a similar method described in Sec. II B. The

energy loss due to the lattice matching (E_{loss}) is large [$24 \text{ meV}/(\text{BCN})_2$] since we have one graphene layer for two h -BN layers. The in-plane lattice constant (2.462 \AA) here is also larger than those of the thin films in the previous subsections, and closer to that of h -BN (2.475 \AA in a LDA calculation).

Figure 6 shows the band structure of the $aBaa'Ca'$ -stacking and the $aBcc'Ab$ -stacking thin films. The $aBaa'Ca'$ -stacking thin film has a band gap of 99 meV while the $aBcc'Ab$ -stacking thin film has almost linear and gapless dispersion. The equivalence of the two carbon sublattices in graphene is broken in the $aBaa'Ca'$ -stacking thin film, but that in the $aBcc'Ab$ -stacking thin film is preserved. These geometrical differences determine a band gap as discussed in Sec. III B. However, in contrast to the graphene/ h -BN monolayer thin film cases, the overlap between the states in two graphene layers (intergraphene interactions) is almost negligible because of the existence of two h -BN layers. Thus, the electronic structures of the graphene/ h -BN bilayer thin films can be discussed by considering only the sublattice symmetry breaking.

IV. SUMMARY

We find the layer-number dependence of the total energy (inversely proportional to the layer number) and the band gap (monotonic reduction) of graphene/ h -BN monolayer thin films. We show that four or more layers are needed to make the lattice-matched thin films stable based on the simulation of lattice-mismatched thin films by considering twisted thin films. The band gaps of these thin films are determined by the overlap among the states of different graphene layers. We also demonstrate the gap modulation by using the electric field caused by the alteration of the relative potential energy. Finally, we suggest six-layer graphene/ h -BN bilayer thin films with a finite band gap or a linear dispersion relation depending on the stacking patterns. These six-layer thin films should be ideal for applications because the graphene layers are protected by h -BN layers.

ACKNOWLEDGMENTS

All numerical calculations were carried out on the TSUB-AME2.0 supercomputer in the Tokyo Institute of Technology. This work was supported by NSF Grant No. DMR-10-1006184, and the theory program at the Lawrence Berkeley National Laboratory through the Office of Basic Science, U. S. Department of Energy under Contract No. DE-AC02-05CH11231. Y.S. acknowledges financial support from Japan Society for the Promotion of Science (JSPS, 12J08928). S.S. acknowledges the financial support by Grant-in-Aid for Scientific Research from JSPS (Grant No. 25107005), Global COE Program of MEXT Japan through the Nanoscience and Quantum Physics Project of the Tokyo Institute of Technology, and MEXT Elements Strategy Initiative to Form Core Research Center through Tokodai Institute for Element Strategy.

[1] C. R. Dean, A. F. Young, I. Meric, C. Lee, L. Wang, S. Sorgenfrei, K. Watanabe, T. Taniguchi, P. Kim, K. L. Shepard, and J. Hone, *Nat. Nanotechnol.* **5**, 722 (2010).

[2] R. Decker, Y. Wang, V. W. Brar, W. Regan, H.-Z. Tsai, Q. Wu, W. Gannett, A. Zettl, and M. F. Crommie, *Nano Lett.* **11**, 2291 (2011).

- [3] N. Kharche and S. K. Nayak, *Nano Lett.* **11**, 5274 (2011).
- [4] B. Sachs, T. O. Wehling, M. I. Katsnelson, and A. I. Lichtenstein, *Phys. Rev. B* **84**, 195414 (2011).
- [5] M. Kindermann, B. Uchoa, and D. L. Miller, *Phys. Rev. B* **86**, 115415 (2012).
- [6] J. C. W. Song, A. V. Shytov, and L. S. Levitov, *Phys. Rev. Lett.* **111**, 266801 (2013).
- [7] M. Yankowitz, J. Xue, D. Cormode, J. D. Sanchez-Yamagishi, K. Watanabe, T. Taniguchi, P. Jarillo-Herrero, P. Jacquod, and B. J. Leroy, *Nat. Phys.* **8**, 382 (2012).
- [8] C. R. Dean, L. Wang, P. Maher, C. Forsythe, F. Ghahari, Y. Gao, J. Katoch, M. Ishigami, P. Moon, M. Koshino, T. Taniguchi, K. Watanabe, K. L. Shepard, J. Hone, and P. Kim, *Nature (London)* **497**, 598 (2013).
- [9] B. Hunt, J. D. Sanchez-Yamagishi, A. F. Young, M. Yankowitz, B. J. LeRoy, K. Watanabe, T. Taniguchi, P. Moon, M. Koshino, P. Jarillo-Herrero, and R. C. Ashoori, *Science* **340**, 1427 (2013).
- [10] M. Mucha-Kruczyński, J. R. Wallbank, and V. I. Fal'Ko, *Phys. Rev. B* **88**, 205418 (2013).
- [11] L. A. Ponomarenko, R. V. Gorbachev, G. L. Yu, D. C. Elias, R. Jalil, A. A. Patel, A. Mishchenko, A. S. Mayorov, C. R. Woods, J. R. Wallbank, M. Mucha-Kruczyński, B. A. Piot, M. Potemski, I. V. Grigorieva, K. S. Novoselov, F. Guinea, V. I. Fal'Ko, and A. K. Geim, *Nature (London)* **497**, 594 (2013).
- [12] G. Giovannetti, P. A. Khomyakov, G. Brocks, P. J. Kelly, and J. van den Brink, *Phys. Rev. B* **76**, 073103 (2007).
- [13] J. Sławińska, I. Zasada, and Z. Klusek, *Phys. Rev. B* **81**, 155433 (2010).
- [14] J. Sławińska, I. Zasada, P. Kosiński, and Z. Klusek, *Phys. Rev. B* **82**, 085431 (2010).
- [15] A. Ramasubramaniam, D. Naveh, and E. Towe, *Nano Lett.* **11**, 1070 (2011).
- [16] X. Zhong, Y. K. Yap, R. Pandey, and S. P. Karna, *Phys. Rev. B* **83**, 193403 (2011).
- [17] R. Balu, X. Zhong, R. Pandey, and S. P. Karna, *Appl. Phys. Lett.* **100**, 052104 (2012).
- [18] E. Kan, H. Ren, F. Wu, Z. Li, R. Liu, C. Xiao, K. Deng, and J. Yang, *J. Phys. Chem. C* **116**, 3142 (2012).
- [19] X. Zhong, R. G. Amorim, R. H. Scheicher, R. Pandey, and S. P. Karna, *Nanoscale* **4**, 5490 (2012).
- [20] Y. Sakai, T. Koretsune, and S. Saito, *Phys. Rev. B* **83**, 205434 (2011).
- [21] Y. Sakai and S. Saito, *J. Phys. Soc. Jpn.* **81**, 103701 (2012).
- [22] O. M. Nayfeh, A. G. Birdwell, C. Tan, M. Dubey, H. Gullapalli, Z. Liu, A. L. M. Reddy, and P. M. Ajayan, *Appl. Phys. Lett.* **102**, 103115 (2013).
- [23] S. Roth, F. Matsui, T. Greber, and J. Osterwalder, *Nano Lett.* **13**, 2668 (2013).
- [24] L. Britnell, R. V. Gorbachev, R. Jalil, B. D. Belle, F. Schedin, A. Mishchenko, T. Georgiou, M. I. Katsnelson, L. Eaves, S. V. Morozov, N. M. R. Peres, J. Leist, A. K. Geim, K. S. Novoselov, and L. A. Ponomarenko, *Science* **335**, 947 (2012).
- [25] G. Gao, W. Gao, E. Cannuccia, J. Taha-Tijerina, L. Balicas, A. Mathkar, T. N. Narayanan, Z. Liu, B. K. Gupta, J. Peng, Y. Yin, A. Rubio, and P. M. Ajayan, *Nano Lett.* **12**, 3518 (2012).
- [26] P. Hohenberg and W. Kohn, *Phys. Rev.* **136**, B864 (1964).
- [27] W. Kohn and L. J. Sham, *Phys. Rev.* **140**, A1133 (1965).
- [28] D. M. Ceperley and B. J. Alder, *Phys. Rev. Lett.* **45**, 566 (1980).
- [29] J. P. Perdew and A. Zunger, *Phys. Rev. B* **23**, 5048 (1981).
- [30] J. Ihm, A. Zunger, and M. L. Cohen, *J. Phys. C: Solid State Phys.* **12**, 4409 (1979).
- [31] M. L. Cohen, *Phys. Scr. T* **1**, 5 (1982).
- [32] N. Troullier and J. L. Martins, *Phys. Rev. B* **43**, 1993 (1991).
- [33] P. Giannozzi, S. Baroni, N. Bonini, M. Calandra, R. Car, C. Cavazzoni, D. Ceresoli, G. L. Chiarotti, M. Cococcioni, I. Dabo, A. Dal Corso, S. de Gironcoli, S. Fabris, G. Fratesi, R. Gebauer, U. Gerstmann, C. Gougoussis, A. Kokalj, M. Lazzeri, L. Martin-Samos, N. Marzari, F. Mauri, R. Mazzarello, S. Paolini, A. Pasquarello, L. Paulatto, C. Sbraccia, S. Scandolo, G. Sclauzero, A. P. Seitsonen, A. Smogunov, P. Umari, and R. M. Wentzcovitch, *J. Phys.: Condens. Matter* **21**, 395502 (2009).
- [34] H. Rydberg, M. Dion, N. Jacobson, E. Schröder, P. Hyldgaard, S. I. Simak, D. C. Langreth, and B. I. Lundqvist, *Phys. Rev. Lett.* **91**, 126402 (2003).
- [35] D. Vanderbilt, *Phys. Rev. B* **41**, 7892 (1990).
- [36] K. Lee, É. D. Murray, L. Kong, B. I. Lundqvist, and D. C. Langreth, *Phys. Rev. B* **82**, 081101 (2010).
- [37] V. R. Cooper, *Phys. Rev. B* **81**, 161104 (2010).
- [38] L. Bengtsson, *Phys. Rev. B* **59**, 12301 (1999).
- [39] A. Kokalj, *Comput. Mater. Sci.* **28**, 155 (2003).
- [40] Y. Sakai and S. Saito, *Mater. Res. Soc. Symp. Proc.* **1407**, 1407AA0803 (2012).
- [41] J. D. Bernal, *Proc. R. Soc. A* **106**, 749 (1924).
- [42] A. N. Kolmogorov and V. H. Crespi, *Phys. Rev. B* **71**, 235415 (2005).
- [43] J. M. Campanera, G. Savini, I. Suarez-Martinez, and M. I. Heggie, *Phys. Rev. B* **75**, 235449 (2007).
- [44] E. McCann and M. Koshino, *Rep. Prog. Phys.* **76**, 056503 (2013).